Multiple Object Tracking for Occluded Particles

YIFEI QIAN, RU JI, YUPING DUAN, AND RUNHUAI YANG
Department of Biomedical Engineering, Anhui Medical University, Hefei 230022, China

Corresponding authors: Yuping Duan (duanyuping126@126.com) and Runhuai Yang (yangrunhuai@ahmu.edu.cn)

ABSTRACT The precise detection and tracking of multiple particles under a microscope are of significance in the research of the individual and cluster behavior of dynamic bacteria and subcellular structures. However, the existing detection algorithms cannot separate occluded particles from each other, and most of the tracking algorithms aimed to address the occlusion involve several uncertainties. In this paper, a two-step detection algorithm based on the threshold segmentation and morphological open operation has been developed for identify non-fluorescent labeled particles under microscope, which could separate micro-contact targets. Moreover, we have proposed a novel correlation algorithm that can exploit the strengths of the global shortest path algorithm and Hungarian algorithm, which updating online in real time and considering the occlusion among particles. The proposed approach could achieve the temporal optimal match and spatial optimal solution by utilizing the multi-frame information. Moreover, the proposed method could realize the tracking of occluded particles tracking, and outperform the single global shortest path algorithm and Hungarian algorithm. The proposed method was successfully applied to six real image sequences with the maximum number of particles per frame ranging from 23 to 55, as well as a synthetic and fluorescent labeled sequence. The results of the contrast experiments demonstrated that the proposed algorithm is practical and can realize real-time tracking.

INDEX TERMS Microscopic image, multiple particles tracking, target occlusion, global data association.

I. INTRODUCTION

As a key branch of computer vision, object tracking has been widely studied by scholars in recent years. The existing target tracking algorithms primarily involve two stages: detection and data association. Considering the distinction of targets, object tracking can be categorized into two types: non-particle tracking involving abundant features to be learned and particle tracking corresponding to monotonous shapes and textures with no obvious features to be learned. To address the former case, many types of detection algorithms are available, such as those involving frame differences, background subtraction and deep learning. In recent years, deep learning have emerged as popular detection algorithms, such as R-CNNs [1]–[3], YOLOs [4]–[6], SSD [7]. The detection in the latter case is more complex due to the nearly identical appearance of the particles. The relevant common algorithms include threshold segmentation [8] and spot enhanced filter (SEF) [9]–[12], which is the most widely employed technique.

Biological particles including bacteria, cells, viruses, microtubules [9], [10], [13], [14], are generally observed through a microscope. The automatic detection and tracking of the particles can reduce the workload of scientific researchers, as several of these tasks cannot be accomplished manually. However, the precision of the detection and tracking directly affects the accuracy of the research results. Because of the diversities in the observation platforms, the images obtained directly usually contain a considerable amount of impurities and noise. A specific technique to realize denoising is to highlight the target particles through a fluorescent mark. And most of the existing studies are focused on the detection and tracking of fluorescent labeled particles. In contrast, the present study is focused on the non-fluorescent labeled particles. In general, the nonfluorescent labeled particles exhibit a similar appearance. Moreover, a considerable amount of noise, with a morphology similar to that of the particles, is present in the background, known as the ''pseudo particle''. In addition, other challenges to particle tracking include immeasurability of motion, appearance and disappearance, aggregation, overlap and occlusion.

Previous particle tracking can be divided into deterministic and probabilistic methods. The former is composed of

The associate editor coordinating the review of this manuscript and approving it for publication was G R Sinha.

target detection and data association. As temporal and spatial uncertainties are discarded, the tracking usually struggles with complicated situation. The latter consists of object detection, state forecast and data association, and the tracking performance is enhanced when considering the temporal and spatial uncertainties. For approach that only considers spatio-temporal uncertainties between two successive frames [15], they usually encounter the challenge of limited temporal information. Furthermore, the methods that consider the information of multiple frames often throw away the spatial messages [10].

As mentioned previously, the algorithm that is most commonly applied to detect fluorescent labeled particles is the spot enhanced filter. In [9], spot enhanced filter and specified area sampling were applied in a joint manner to detect targets, and the probability in the PDA was considered as the likelihood weight of the image for correlation. In [10], to detect multi-scale particles, multiple standard deviations of spot enhanced filter and two-step multi-frame association were adopted.

For multiple particles tracking, the key challenge is to address the occlusion among particles as it confuses detection algorithms, causing the algorithms to treat multiple occluded particles as one particle. To the best of our knowledge, none of the existing detection algorithms can distinguish among the occluded particles. And data association algorithms must be used to process the occlusions. In [9], adjacent support of each image location relative to tracked target was calculated, and the support was used to recalculate the weights of PDA. This methodology could accomplish object clustering but could not process the occlusion among the targets. In [13], the dummy particle of a vanishing or occluded particle was simulated (this step does not need to be implemented in the proposed approach), and the dummy particle was assigned an extremely small probability value. The purpose was to ensure the continuity of the trajectory until the appropriate correlation occurred; however, the instance at which the appropriate correlation occurred and the optimality of this correlation were not clarified in the article. In [12], a tracking tree was established and dummy particles were synthesized for each particle in next frame. Moreover, the four closest particles in the next frame were added to the branch of the particle such that one particle had five particles associated with it in the next frame. However, this approach involved a considerable amount of uncertainties, and the calculation increased.

To detect non-fluorescent particles, we have proposed a two-step detection method based on threshold segmentation and morphological operation to separate micro-contact targets. First, the foreground is extracted from the background through the threshold segmentation, and subsequently, the morphological operation is performed to separate targets with slight contact to ensure the accuracy of detection and tracking. The advantage of threshold segmentation is that the particles with different scales in the same image can be detected without other additional operations, while spot
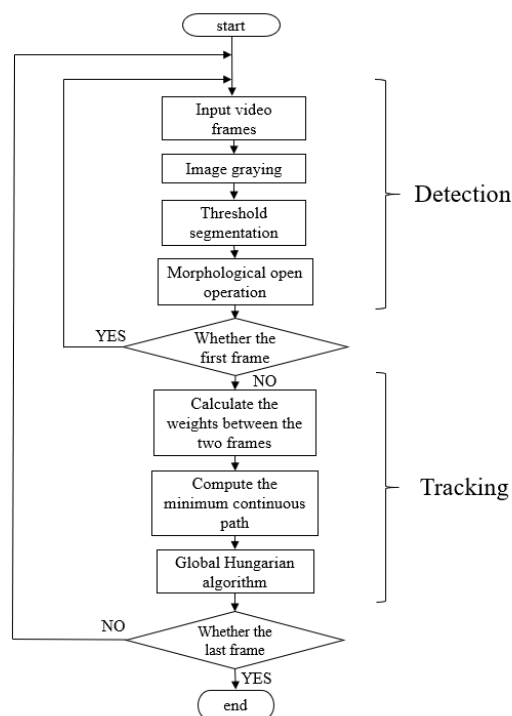

FIGURE 1. Algorithm flowchart.

enhanced filter is restricted to the standard deviation of the Gaussian filter.

Moreover, we have developed a new data association method based on global shortest path algorithm and Hungarian algorithm. The Hungarian algorithm pairs in a bipartite graph, considering the information between two successive frames in the tracking process. However, to realize the spatial optimal matching, the algorithm ignores the abundant information in the past and future frames. In contrast, the global shortest path algorithm realizes the optimal solution in time and neglect the spatial optimization. In this paper, the advantages of the both algorithms are integrated to effectively address the occlusion between particles. To the best of our knowledge, this is the first time to utilize a spatially and optimally optimal solution to address the particles occlusion problem, rather than relying on the considerable uncertainties. The process flow of the algorithm is illustrated in Fig. 1.

The rest of the paper is organized as follows. The second and third sections describe the target detection algorithm and novel data association algorithm, respectively. The fourth section describes the experiments, and the fifth section presents the concluding remarks.

II. PARTICLES DETECTION
This section describes the detection algorithm for the fluorescent and non-fluorescent particles. First, we describe the most commonly used technique, that is, the spot enhanced filter approach, and later elaborate upon the proposed method to detect the nonfluorescent particles.

A. SPOT ENHANCED FILTER

Spot enhanced filter, also known as Laplace of Gaussian filter (LoG), is the most widely used approach to detect fluorescent labeled particles and is one of the most effective algorithms [10]. LoG was originally employed to enhance edge information in image processing. Due to the nature of particle detection, the particles usually appear as a simple "spot" under fluorescence microscope, which can be regarded as edge to some extent. Spot enhanced filter detect particles with a fixed scale, and therefore, the parameters must be adjusted to adapt to different particle sizes. Nevertheless, in [10], multiple Gaussian standard deviations were taken to achieve multi-scale particle detection, similar to the image pyramid.

The convolution kernel of spot enhanced filter can be expressed as (1) [10], [14], where x and y are the horizontal and vertical coordinates of image, respectively, and σ represents the Gaussian standard deviation.

$$\text{LoG}(x, y, \sigma) = \frac{x^2 + y^2 - 2\sigma^2}{2\pi\sigma^6} e^{\frac{-(x^2+y^2)}{2\sigma^2}} \quad (1)$$

A threshold is necessary for images after LoG to extract particles and eliminate noise [9].

B. THRESHOLD SEGMENTATION AND MORPHOLOGICAL OPERATION

To detect the non-fluorescent labeled particles, considering the diverse target intensities and considerable amount of background noise, we have proposed a two-step detection algorithm based on threshold segmentation and morphological operation. As the simplest image processing operation, threshold segmentation is powerful, in accordance with Occam's razor law, which states that "the simpler, the more effective" [24]. Compared with other algorithms, threshold segmentation has merits of accurate positioning, small computation, simple principle implementation [25], etc., which is suitable for images with considerable differences among foreground and background. The formula can be expressed as (2), where $g(x)$ and $f(x)$ represent the image before and after thresholding, respectively, and a is the threshold that can be artificially assigned or automatically determined [16].

$$f(x) = \begin{cases} 0, & g(x) < a \\ 1, & g(x) > a \end{cases} \quad (2)$$

After thresholding, we employ corrosion or open in morphological operation to separate micro-contact targets, as the second step of the proposed detection to reduce the burden of the follow-up and enhance the tracking accuracy. The corrosion formula can be expressed as (3) [23]. In particular, for a moving structural element B, if the intersection of B and A is all in the effective region of A (A is usually the image to be processed), the central point is saved. The set of all points meeting the conditions is the result of structure A being corroded by structure B.

$$A \odot B = \{x | Bx \subseteq A\} \quad (3)$$
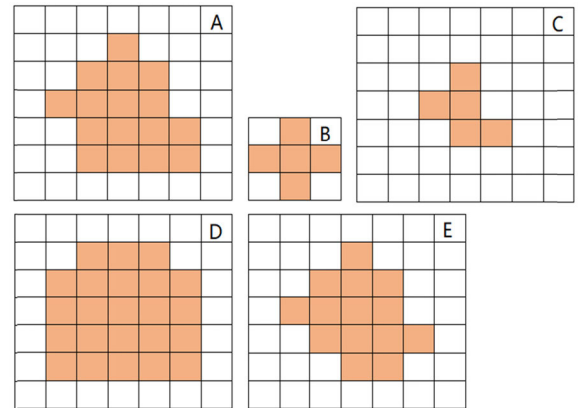
FIGURE 2. Morphological operations diagram. A is the original image; B represents the morphological structure with a kernel size of 3 × 3; C is the result after corrosion; D is the consequence of inflation; E denotes the image after open operation.

The inflation operation equation can be expressed as (4) [23], and considered as the convolution operation of structure B on structure A. If an overlap region exists between structure B and structure A in the process of moving structure B, the location is recorded. The set of all positions involving the intersection of the moving structure B and structure A is the result of inflation of structure A under the action of structure B.

$$A \oplus B = \{z | (B \wedge)z \cap A \neq \emptyset\} \quad (4)$$

In this paper, we employ the open operation as the post-processing operation for detection. The open operation involves first corroding and later inflating the image to remove the noise and separate the targets with a slight contact. The results of corrosion, expansion, and open operation are shown in Fig. 2.

III. MULTIPLE PARTICLES TRACKING

This section describes multiple particles tracking algorithm. We first introduce the concept of graph model and latter explain the principle of global shortest path algorithm and Hungarian algorithm respectively. Finally, the proposed algorithm is explained.

A. GRAPH MODEL

The graph model [17] is made up of nodes and edges, with each node representing one or a group of variables and the edge bearing the contact information between nodes representing the bridge between connecting nodes. In the case of particle tracking, the object detected in successive frames can be regarded as the nodes of the graph model. According to the relationship between particles in different frames, we selectively establish the correlation between them. A graph model can be grouped into directed graph model and undirected graph model. The edges of the former and latter models are connected and not connected in a directional manner, respectively. We consider a directed graph model to represent our network as a certain orientation exists, stemming from the previous image to the next.

B. GLOBAL SHORTEST PATH ALGORITHM

From a node to another node along the edge of a graph, the path with the minimum sum of weights on each edge is the shortest path. In particle tracking, the weight of the edge refers to the cost between two particles. We choose Dijkstra [18] to obtain the shortest path between two nodes. The Dijkstra calculates the shortest path from the starting vertex to the specified node using a greedy strategy. Specifically, the algorithm gradually increasing the weight of the shortest path by selecting the vertex closest to the starting node until all the node in the graph are covered, thereby achieving the optimal solution between two vertices in time dimension.

C. HUNGARIAN ALGORITHM

The Hungarian algorithm is a combinatorial optimization algorithm used to solve linear assignment problem in polynomial time. The algorithm can achieve the maximum matching of two vertex sets in a bipartite graph and concurrently ensure the minimum matching loss sum [15]. Two sets of vertices are considered: $V1 = \{X1, X2, X3\} V2 = \{Y1, Y2, Y3, Y4\}$, with $X1-X3$ represents the three vertices in $V1$ and $Y1-Y4$ represents the four vertices in $V2$. $V1, V2$ connected through $E = \{(X1, Y2, C1), (X1, Y4, C2), (X2, Y1, C3), (X2, Y3, C4), (X3, Y2, C5)\}$, where C represents the loss between two vertices. The objective of the Hungarian algorithm is to minimize the total loss of the connections while ensuring the maximum match 3 between $V1$ and $V2$. The algorithm achieves the spatially optimal solution of the targets. As the Hungarian algorithm only considers the temporal information between two successive frames, which is finite [10], the algorithm cannot realize accurate correlations in complex scenes such as overlap and occlusion. As mentioned previously, this aspect is a challenge for most data association algorithms.

D. OUR PROPOSALS

The global shortest path algorithm often neglects the spatial optimum while achieving the global optimal solution temporally. The Hungarian algorithm is the other way around. We consider combining the two methods in a complementary manner. The proposed tracking techniques are described in the following text.

Euclidean distance between the object is considered as the similarity measurement. Because the considered targets are particles with similar appearance, with similar shapes and scales, the cost based on *physical property* proposed in [13] does not satisfy our requirements. In each frame, we acquire several measured particles $\{p_k^i\}$ after detection, where k denotes the k-th frame, and i represents the i-th detected particle in the k-th frame. In order to distinguish particles of different frames, we place the detected particles of each frame on different layers of the graph model. Only the particles in successive layers can be pair with each other, and the set of particles of each layer is represented by H. Before calculating the similarity measurement, we design a circular tracking gate for each particle in the following frame. The particle in the next frame can contact particles in the previous
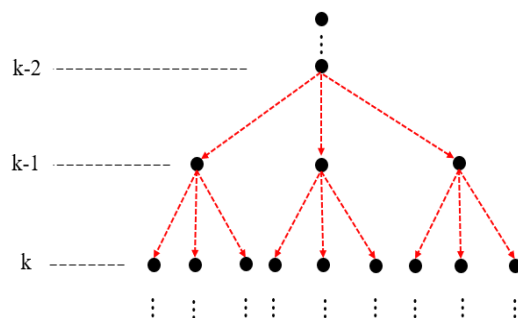

FIGURE 3. k-2, k-1, and k are three sequential frames which represent three successive layers in the tracking graph. k-2 can only connects with k-1 downward, and k-1 connect with k in same way. When particles in the next frame fall into tracking gate, they are eligible to contact with the current particle.

frame only if it falls into the tracking gate, as shown in Fig. 3. The function of tracking gate is to remove the particles that are clearly unrelated. This mechanism can reduce the interference between particles and the cost of computation. As soon as the correlation between the particles is set up, the similarity measurement between the particles is computed. Unlike the Hungarian algorithm, which only determines the loss between two successive frames, we compute the loss between multiple frames. To ensure consistent updating, we introduce a sliding window $(k - t \rightarrow k)$ in the temporal dimension, with the time step specified as t, to obtain fixed number (t) of frames addressed each time. Subsequently, the losses of continuous path of particles from the $k - t$ frame to the k frame are computed, and discontinuous points are neglected. In contrast, in two-frame tracking method, only the relations in two frames are considered [11]. For each pair of particles from p_{k-t}^i to p_k^j, we tentatively elect the one with minimum consecutive loss as the path, calculated by Dijkstra algorithm. Until now, we have completed optimal matching between point and point from $k - t$ to k frame. To pursue global optimization, we comprehensively process all particles in $k - t$-th and k-th frame. We regard targets of $k - t$-th frame and k-th frame as the two parts in bipartite graph, and employ the Hungarian algorithm to seek for optimal solution. When confronted with occlusion, the occluded particles are captured as soon as particles separate from each other because the proposed algorithm is optimal at all times. Although the Hungarian algorithm only pairs targets between the first and the last frame on sliding window one to one, when the window slides along the timeline, the overlapped and occluded particles inside can be matched twice, as shown in Fig. 4. We call this method the "global Hungarian algorithm".

IV. EXPERIMENTAL RESULTS ADN DISCUSSION

In this chapter, we first describe the experiment and evaluation of particle detection. Then we introduce the new tracking algorithm used to realize the particle tracking in simulation and real scenarios. Subsequently, we compare the common SEF and two step SEF, and finally, we compare the two step SEF with the proposed algorithm. All the experiments are based on python 3.6.5.
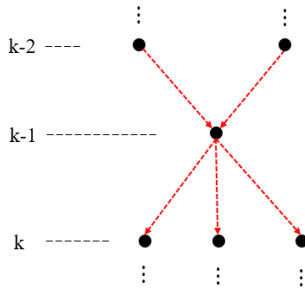
FIGURE 4. Particle occlusion occurs in the k-1 frame. The two particles in k-2 are detected as only one in k-1. However, as the occluded particle falls into two tracking gates in k-2, it establishes a correlation with both particles. On the time sliding window (for convenience, we consider the time step t as 2), we determine the optimal match between k-2 and k to solve the occlusion problem.

## A. PARTICLE DETECTION EXPERIMENTS AND EVALUATION

Because the fluorescent labeled particles often appear as a spot under a microscope, the spot enhanced filter exhibits a high detection performance. In contrast, for non-fluorescent labeled particles, the detection effects of direct threshold segmentation and spot enhanced filter are nearly equivalent. Spot enhanced filter can easily detect noise in the background. Considering these aspects, we recommended the separation of the foreground and background directly through the threshold segmentation to realize the detection in fluorescent labeled images. In the following analysis of both the spot enhanced filter and direct threshold segmentation, morphological operation could be used as the second step of detection, i.e., post-detection, to separate targets with slight contact. We first detected particles with spot enhanced filter and direct threshold segmentation severally, and later performed morphological open operation.

We performed an exploratory experiment on an image with micro-contact between particles. For spot enhanced filter, we smoothed the image with a Gaussian filter and enhanced the particles through a Laplace filter. Next the threshold segmentation and morphological open operation were performed. The standard deviation of the Gaussian filter was 0; the size of the Gaussian kernel and Laplace filter kernel were 17×17 and 5×5, respectively; the threshold value was 91, and the scale of the open operation kernel was 3×3. In direct threshold segmentation, the threshold value was 91, and the kernel size of open operation was 3×3. The experimental results are shown in Fig. 5. Both spot enhanced filter and direct threshold segmentation can achieve the separation of slight contact targets after open operation. In addition, open operation eliminates certain noise in the original image after thresholding. Therefore, it is desirable to employ open operation for post-detection in particles detection.

We collected two sequences of non-fluorescent labeled bacteria under microscope, called Scenario 1 and Scenario 2, with the maximum number of particles per frame being 23 and 55, respectively. For Scenario 1 and Scenario 2, we harnessed the common spot enhanced filter, spot enhanced filter with open operation and the proposed detection algorithm based on threshold segmentation to detect the particles.
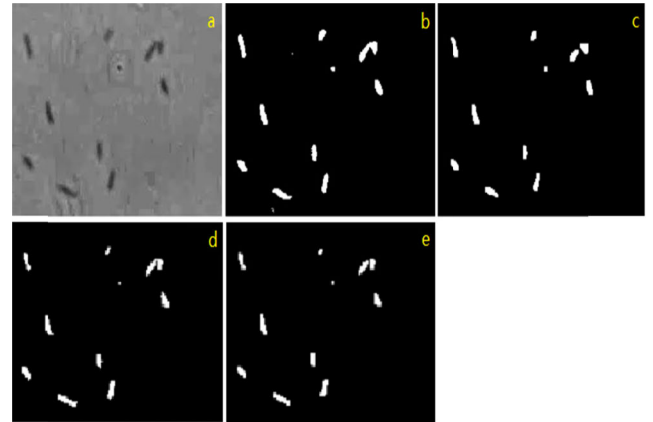
FIGURE 5. Detection comparison. a is the raw image; b is the consequence of LoG after thresholding, including a certain amount of noise; c is the result of spot enhanced filter after open operation; d is the result of direct threshold segmentation, e is the open operation consequence of d.
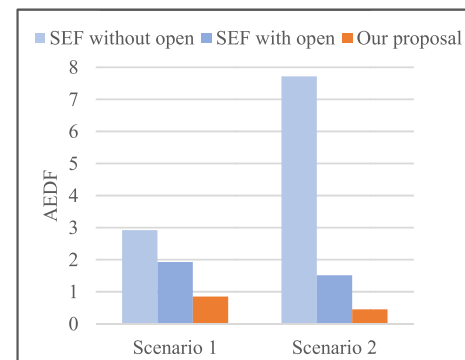
FIGURE 6. Average number of false particles per frame.

We calculated the corresponding average error detection per frame (AEDF), accuracy rate and recall rate. The accuracy rate and recall rate were calculated using the expressions shown as (5) and (6), respectively [19].

$$P = \frac{TP}{TP + FP} \tag{5}$$

$$R = \frac{TP}{TP + FN} \tag{6}$$

where TP is the total number of correctly detected particles, FP represents the number of false particles, and FN is the count of undetected particles that are mistaken as noise or background. The statistical results are shown in Fig. 6, 7 and 8. It can be seen that the proposed detection is superior to the other two methods under the same recall rate.

B. NON-FLUORESCENT LABELED PARTICLE TRACKING EXPERIMENTS AND EVALUATION

To verify the feasibility of the proposed algorithm, particle tracking was conducted in synthetic and real scenarios. In the synthetic, the number of particles was restrained to six, and the particles moved randomly. Severe occlusions occurred between the particles, which was the objective for developing this scene. Because the simulation scenario was
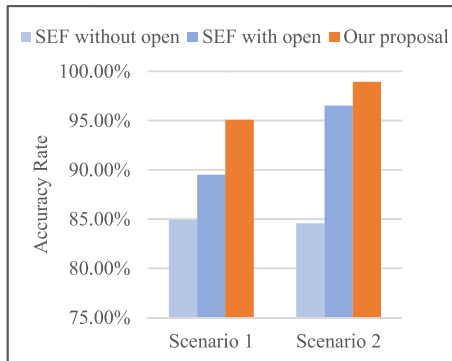
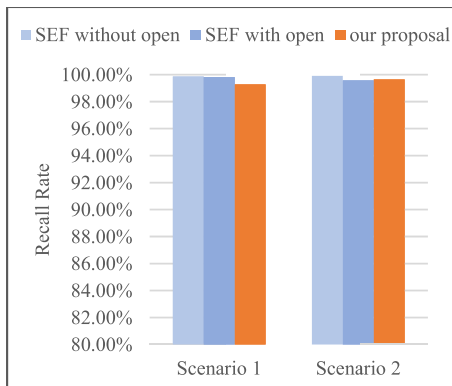**FIGURE 7.** Statistics of the detection accuracy rate.

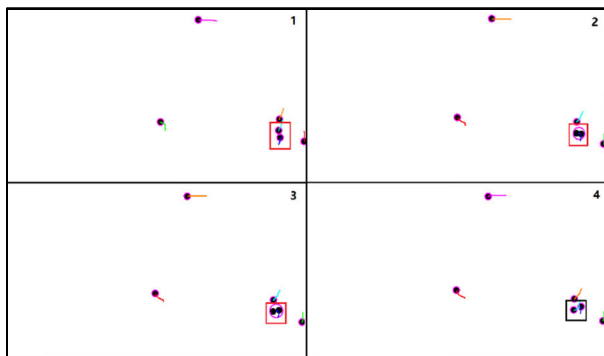**FIGURE 8.** Statistics of the detection recall rate.

FIGURE 9. 1-4 are four consecutive frames. Occlusion occurs in 2-3 frames, and in the fourth frame, the two occluded particles are separated and tracked.

aimed at demonstrating the feasibility of the proposed tracking algorithm, we did not compare the proposed tracking algorithm with the existing tracking algorithms. Tracking was performed based on the result of direct threshold segmentation and open operation. In the experiment, we observed the particle tracking and determined the tracking accuracy. The tracking results and tracking accuracy are shown in the Fig. 9 and Table 1, respectively.

The consequences of the synthetic scene show that the proposed tracking algorithm is feasible. Next, we applied the algorithm in real scenarios to examine the tracking performance. The real scenarios were image sequences observed

TABLE 1. Comparison of the tracking accuracy.

Scenarios	Tracking results		
	Hungarian algorithm	Global shortest path algorithm	Our proposal
Synthesis	—	—	**99.37%**
Scenario 1	81.25%	93.68%	**96.68%**
Scenario 2	68.85%	81.62%	**91.26%**
Scenario 3	82.68%	84.47%	**96.90%**
Scenario 4	80.50%	82.89%	**96.65%**
Scenario 5	73.19%	84.50%	**92.61%**
Scenario 6	77.94%	81.76%	**92.50%**

under microscope with non-fluorescent mark. In addition to Scenario 1 and Scenario 2, we collected another four real scenarios numbered Scenario 3,4,5,6. We performed tracking in Scenario 1-6 with the maximum number of particles per frame were 23 to 55. To the best of our knowledge, the number of particles per frame targeted by most particle tracking algorithms is less than 30. Likewise, the motions of particles could not be measured. The proposed method was compared with the global shortest path algorithm and Hungarian algorithm. Neither the global shortest path nor Hungarian algorithm could process the occluded particles, and the algorithms failed to comprehensively consider the temporally and spatially global information. Our algorithm effectively processed the particle occlusion. Consequently, the algorithm could effectively address complex situations and outperformed the single global shortest path algorithm and Hungarian algorithm. In this paper, the similarity measurements of global shortest path algorithm and Hungarian algorithm were based on the Euclidean distance. For the global shortest path algorithm, we set the step size of the sliding window as 10, and then searched out the shortest distance between frames to accomplish tracking. The Hungarian algorithm only calculated the loss between two successive frames and later determined the maximum matching between particles in the two frames, while ensuring the minimum sum of losses. We quantitatively analyzed of these three methods and calculated their correct tracking rates. The correct tracking rate was calculated using (7) [10], where N_{error} represents the number of errors in tracking, and N_{total} is the total number of particles.

$$P_{correct} = 1 - \frac{N_{error}}{N_{total}} \qquad (7)$$

For the six real scenarios, we first utilized the two-step detection algorithm based on threshold segmentation and open operation to extract particles from background and obtained the coordinate of particles. The threshold value for Scenario 1 to Scenario 6 were 80, 93, 60, 53, 56 and 60, respectively. Next, the Hungarian algorithm, global shortest path algorithm and the proposed method were applied to track the particles. The cost of the Hungarian algorithm was the loss between predicted states of the current frame particles and the measured states. Kalman filter [19], [20] was used to estimate
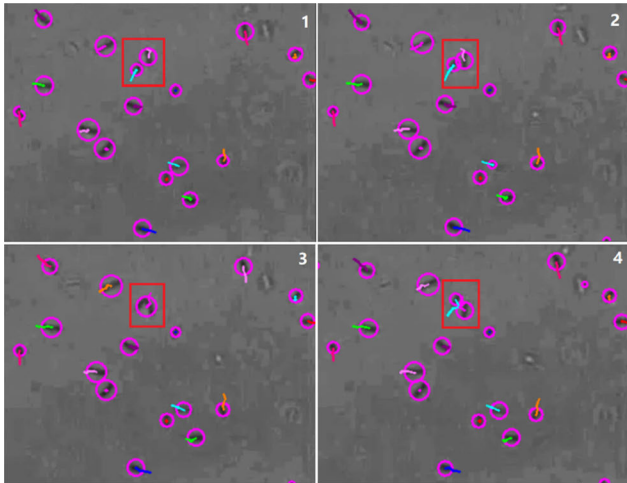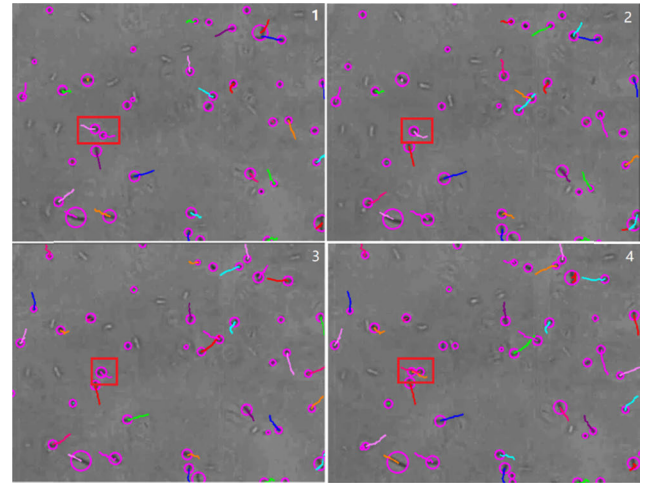
FIGURE 10. Tracking consequence of the proposed algorithm applied to Scenario 1.

FIGURE 11. Tracking consequence of the proposed algorithm applied to Scenario 2.

the states. For the proposed and global shortest path algorithm, the states were not estimated. The comparison results of the three tracking algorithms are presented in Table 1. The tracking accuracies of the three methods are nearly more than 70%, which can satisfy the requirements of multiple object tracking basically. However, the performance of Hungarian algorithm is unstable, hovering between 68.85% and 82.68%. The accuracy of global shortest path algorithm is higher than 80%, which corresponds to a satisfactory performance. Nevertheless, the performance of our proposals is better than the previous two algorithms, and the tracking accuracy is more than 90%.

Four successive frames from the results of the proposed tracking algorithm applied to Scenario1 and Scenario 2 are show in Fig. 10 and Fig. 11 respectively. In Fig. 10, the particles in the first two frames approach gradually, and occlusion occurs in the third frame. Although occlusion is not processed in the third frame, in the fourth frame, the algorithm is updated online, the particles are detected as soon as they separate from each other, and the occluded particles are re-associated. In Fig. 11, continuous occlusion occurs in the second and the third frame, and in fourth frame, the occluded particles are successfully identified. The particles in the red rectangle in Fig. 10 and Fig. 11 depict our tracking process from gradual approach to occlusion to separation.

C. TWO-STEP SPOT ENHANCED FILTER IN TRACKING

Since the traditional spot enhanced filter did not involve an open operation, we incorporated the open operation after spot enhanced filter to examine the corresponding tracking performance. We first applied the general spot enhanced filter, later implemented the two-step spot enhanced filter, and finally compared the tracking performance of the two algorithms. Two groups of experiments were carried out for fluorescent labeled and non-fluorescent labeled scenarios. In the fluorescent labeling scene, the microtubule snr 7 density data set in Particle Tracking Challenge 2012, were considered, termed as Scenario 7. Scenario 2 was selected for non-fluorescent

TABLE 2. Comparison of the tracking accuracy between two spot enhanced filters.

Scenarios	Spot enhanced filter	
	With open	Without open
Scenario 2	91.09%	89.50%
Scenario 7	96.61%	96.18%

labeled environment. We first considered Scenario 7, and the global Hungarian algorithm we proposed was used for the tracking algorithm. The Gaussian kernel was sized 15×15, the standard deviation of Gaussian was zero, the Laplace filter kernel was sized 5×5, and the final threshold was 65. To evaluate the contribution of the morphological operation in spot enhanced filter, open and no-open operation were employed after thresholding, and the kernel size of open operation was set as 3×3. Since the particles existed only briefly in this dataset, the step size of the sliding window was set as 5. In Scenario 2, kernel of Gaussian filter was 15×15, the standard deviation was 0, the kernel size of Laplace filter was 5×5, the kernel size of the open operation was 3×3, and the final threshold was 90. The sliding window size was 10. The final consequences of tracking accuracy are shown in Table 2. In the fluorescent labeled scene, the effect of the open and no-open operation for the spot enhanced filter is only slightly different, and the tracking accuracy is more than 96%. But in scenario 2, the difference value reaches 1.58%. Therefore, when using the spot enhanced filter to detect particles in non-fluorescent labeled scenario, it is advisable to add an open operation to filter out noise and separate micro-contact targets.

D. COMPARED WITH OUR PROPOSAL

This section compared the open-operation spot enhanced filter with the proposed two-step detection algorithm; both of the approaches are all two-step detection algorithms. The experiments were conducted under Scenario 2 and

TABLE 3. Comparison of the tracking accuracy with our proposed algorithm.

Scenarios	SEF with open	Our proposal
Scenario 2	91.09%	91.26%
Scenario 7	96.61%	96.72%

Scenario 7. The parameters of the two-step spot enhanced filter were the same as those mentioned previously. For the proposed approach, in Scenario 7, the threshold value was 25, the open operation kernel size was 3 × 3, and the step size of sliding window was 5. In Scenario 2, the threshold value of the proposed was 93, the length of sliding window was 10, and the open core size was 3 × 3. The results are shown in Table 3. The tracking performance of the proposed algorithm is a little bit better than the two-step spot enhanced filter, which proves that the proposed detection algorithm is comparable to the current mainstream algorithm.

V. CONCLUSION

In this paper, a two-step detection algorithm based on threshold segmentation and morphological operation was proposed for non-fluorescent labeled particles, providing a solid foundation for the follow-up particle tracking and improving the tracking accuracy. Moreover, we developed a new tracking algorithm, which combined the advantages of global shortest path algorithm and the Hungarian algorithm, thereby effectively solving the problem of particles occlusion and providing a novel train of thought for intricate scenarios. However, The Hungarian algorithm and the global shortest path algorithm are only two media to realize the combination of more time information and space optimal solution, and are not the ultimate goal. We expect that more effective algorithms will be developed in the future. In addition, the proposed "Global Hungarian algorithm" can only handle occlusion between two or three particles. The situation of occlusion of more particles cannot be solved at present and requires further research.

REFERENCES

[1] R. Girshick, J. Donahue, T. Darrell, and J. Malik, "Rich feature hierarchies for accurate object detection and semantic segmentation," in *Proc. IEEE Conf. Comput. Vis. Pattern Recognit.*, Jun. 2014, pp. 580–587.
[2] R. Girshick, "Fast R-CNN," in *Proc. IEEE Int. Conf. Comput. Vis. (ICCV)*, Dec. 2015, pp. 1440–1448.
[3] S. Ren, K. He, R. Girshick, and J. Sun, "Faster R-CNN: Towards real-time object detection with region proposal networks," *IEEE Trans. Pattern Anal. Mach. Intell.*, vol. 39, no. 6, pp. 1137–1149, Jun. 2017.
[4] J. Redmon and A. Farhadi, "YOLO9000: Better, faster, stronger," in *Proc. IEEE Conf. Comput. Vis. Pattern Recognit. (CVPR)*, Jul. 2017, pp. 7263–7271.
[5] J. Redmon, S. Divvala, R. Girshick, and A. Farhadi, "You only look once: Unified, real-time object detection," in *Proc. IEEE Conf. Comput. Vis. Pattern Recognit. (CVPR)*, Jun. 2016, pp. 779–788.
[6] J. Redmon and A. Farhadi, "YOLOv3: An incremental improvement," vols. 2–11, 2018, *arXiv:1804.02767*. [Online]. Available: http://arxiv.org/abs/1804.02767
[7] W. Liu, D. Anguelov, D. Erhan, C. Szegedy, S. Reed, C.-Y. Fu, and A. C. Berg, "SSD: Single shot MultiBox detector," in *Proc. Eur. Conf. Comput. Vis.*, 2015, pp. 21–37.
[8] M. R. Edwards, R. W. Carlsen, J. Zhuang, and M. Sitti, "Swimming characterization of serratia marcescens for bio-hybrid micro-robotics," *J. Micro-Bio Robot.*, vol. 9, nos. 3–4, pp. 47–60, Aug. 2014.
[9] W. J. Godinez and K. Rohr, "Tracking multiple particles in fluorescence time-lapse microscopy images via probabilistic data association," *IEEE Trans. Med. Imag.*, vol. 34, no. 2, pp. 415–432, Feb. 2015.
[10] A. Jaiswal, W. J. Godinez, R. Eils, M. J. Lehmann, and K. Rohr, "Tracking virus particles in fluorescence microscopy images using multi-scale detection and multi-frame association," *IEEE Trans. Image Process.*, vol. 24, no. 11, pp. 4122–4136, Nov. 2015.
[11] R. Spilger, T. Wollmann, Y. Qiang, A. Imle, J. Y. Lee, B. Müller, O. T. Fackler, R. Bartenschlager, and K. Rohr, "Deep particle tracker: Automatic tracking of particles in fluorescence microscopy images using deep learning," *Deep Learn. Med. Image Anal.*, vol. 11045, pp. 128–136, Sep. 2018.
[12] R. Spilger, A. Imle, J.-Y. Lee, B. Müller, O. T. Fackler, R. Bartenschlager, and K. Rohr, "A recurrent neural network for particle tracking in microscopy images using future information, track hypotheses, and multiple detections," *IEEE Trans. Image Process.*, vol. 29, pp. 3681–3694, 2020.
[13] L. Feng, Y. Xu, Y. Yang, and X. Zheng, "Multiple dense particle tracking in fluorescence microscopy images based on multidimensional assignment," *J. Struct. Biol.*, vol. 173, no. 2, pp. 219–228, Feb. 2011.
[14] D. Sage, F. R. Neumann, F. Hediger, S. M. Gasser, and M. Unser, "Automatic tracking of individual fluorescence particles: Application to the study of chromosome dynamics," *IEEE Trans. Image Process.*, vol. 14, no. 9, pp. 1372–1383, Sep. 2005.
[15] H. W. Kuhn, "The Hungarian method for the assignment problem," *Nav. Res. Logistics Quart.*, vol. 2, nos. 1–2, pp. 83–97, Mar. 1955.
[16] N. Chenouard, I. Smal, F. De Chaumont, M. Maška, I. F. Sbalzarini, Y. Gong, J. Cardinale, C. Carthel, S. Coraluppi, M. Winter, and A. R. Cohen, "Objective comparison of particle tracking methods," *Nature Methods*, vol. 11, no. 3, pp. 281–289, Mar. 2014.
[17] S. Torgasin and K.-H. Zimmermann, "An all-pairs shortest path algorithm for bipartite graphs," *Open Comput. Sci.*, vol. 3, no. 4, pp. 149–157, Jan. 2013.
[18] C. Wang, Y. Wang, Y. Wang, C. T. Wu, and G. Yu, "muSSP: Efficient min-cost flow algorithm for multi-object tracking," in *Proc. Conf. Neural Inf. Process. Syst.*, 2019, pp. 425–434.
[19] X. Zhao, S. Yan, and Q. Gao, "An algorithm for tracking multiple fish based on biological water quality monitoring," *IEEE Access*, vol. 7, pp. 15018–15026, 2019.
[20] R. Faragher, "Understanding the basis of the Kalman filter via a simple and intuitive derivation [lecture notes]," *IEEE Signal Process. Mag.*, vol. 29, no. 5, pp. 128–132, Sep. 2012.
[21] N. Imirzian, Y. Zhang, C. Kurze, R. G. Loreto, D. Z. Chen, and D. P. Hughes, "Automated tracking and analysis of ant trajectories shows variation in forager exploration," *Sci. Rep.*, vol. 9, no. 1, pp. 1–10, Dec. 2019.
[22] M. Lu, B. Xu, Z. Jiang, A. Sheng, P. Zhu, and J. Shi, "Automated tracking approach with ant colonies for different cell population density distribution," *Soft Comput.*, vol. 21, no. 14, pp. 3977–3992, Jul. 2017.
[23] D. Chudasama, T. Patel, S. Joshi, and G. I. Prajapati, "Image segmentation using morphological operations," *Int. J. Comput. Appl.*, vol. 117, no. 18, pp. 16–19, May 2015.
[24] A. Blumer, A. Ehrenfeucht, D. Haussler, and M. K. Warmuth, "Occam's razor," in *Proc. Int. Conf. Neural Inf. Process. Syst. (NIPS)*, 2000, pp. 276–282.
[25] E. Cuevas, D. Zaldivar, and M. Pérez-Cisneros, "A novel multi-threshold segmentation approach based on differential evolution optimization," *Expert Syst. Appl.*, vol. 37, no. 7, pp. 5265–5271, Jul. 2010.

YIFEI QIAN received the bachelor's degree in engineering from the School of Life Sciences, Anhui Medical University, in 2019, where he is currently pursuing the master's degree with the Department of Biomedical Engineering. His research interests include particle tracking based on computer vision, and object detection based on machine learning.
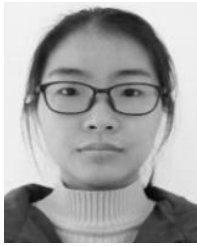
RU JI received the bachelor's degree from the School of Life Sciences, Anhui Medical University, in 2019, where she is currently pursuing the master's degree with the Department of Biomedical Engineering. Her research interests include image processing, and delineation of lesions based on deep learning.

RUNHUAI YANG received the Ph.D. degree from the Robotics Laboratory, Department of Precision Instruments, School of Engineering Science, University of Science and Technology of China (USTC), in 2015.

He is currently working as an Associate Professor with the Department of Biomedical Engineering, Anhui Medical University. His research interests include the development of intelligent soft robot systems, and the development of multi-functional endoscopic surgery robot.

• • •
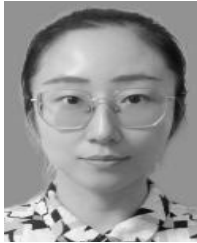
YUPING DUAN received the D.E. degree from the School of Biological Science and Medical Engineering, Southeast University, in 2017.

She is currently working as an Assistant Professor with the Department of Biomedical Engineering, Anhui Medical University. Her research interests include medical image processing based on artificial intelligence, medical information security, and forensics.